

## Research



**Cite this article:** Banack SA, Dunlop RA, Cox PA. 2020 An miRNA fingerprint using neural-enriched extracellular vesicles from blood plasma: towards a biomarker for amyotrophic lateral sclerosis/motor neuron disease. *Open Biol.* **10**: 200116. <http://dx.doi.org/10.1098/rsob.200116>

Received: 29 April 2020

Accepted: 22 May 2020

### Subject Area:

neuroscience/cellular biology

### Keywords:

biomarkers, neurodegeneration, exosomes, miRNA, ALS/MND

### Author for correspondence:

Paul Alan Cox

e-mail: [paul@ethnomedicine.org](mailto:paul@ethnomedicine.org)

Electronic supplementary material is available online at <https://doi.org/10.6084/m9.figshare.c.5015282>.

# An miRNA fingerprint using neural-enriched extracellular vesicles from blood plasma: towards a biomarker for amyotrophic lateral sclerosis/motor neuron disease

Sandra Anne Banack, Rachael Anne Dunlop and Paul Alan Cox

Brain Chemistry Labs, Institute for Ethnomedicine, PO Box 3464, Jackson, WY 83001, USA

PAC, 0000-0001-6401-2981

Biomarkers for amyotrophic lateral sclerosis/motor neuron disease (ALS/MND) are currently not clinically available for disease diagnosis or analysis of disease progression. If identified, biomarkers could improve patient outcomes by enabling early intervention and assist in the determination of treatment efficacy. We hypothesized that neural-enriched extracellular vesicles could provide microRNA (miRNA) fingerprints with unequivocal signatures of neurodegeneration. Using blood plasma from ALS/MND patients and controls, we extracted neural-enriched extracellular vesicle fractions and conducted next-generation sequencing and qPCR of miRNA components of the transcriptome. We here report eight miRNA sequences which significantly distinguish ALS/MND patients from controls in a replicated experiment using a second cohort of patients and controls. miRNA sequences from patient blood samples using neural-enriched extracellular vesicles may yield unique insights into mechanisms of neurodegeneration and assist in early diagnosis of ALS/MND.

## 1. Background

Neurodegenerative diseases such as Alzheimer's disease (AD), Parkinson's disease (PD) and amyotrophic lateral sclerosis/motor neuron disease (ALS/MND) continue to provide challenges for diagnosis since validated, clinically useful diagnostic biomarkers are currently unavailable. Rapid diagnosis and intervention in the disease process could be beneficial in slowing neurodegenerative disease progression as well as facilitating the testing of new therapies. In ALS/MND, the average time from diagnosis to death is typically short (2–5 years) and it is not unusual for patients to wait a year before receiving a diagnosis [1]. Since disease progression correlates with motor neuron loss, early intervention could be critical for the development of new effective drug therapies. Current investigative drugs suggest some hope to reduce the rate of ALS/MND disease progression [2]; however, the discovery of biomarkers would be a tremendous asset to these efforts.

To date, an ALS/MND diagnosis is based on clinical features with the elimination of alternative diagnoses and supporting data retrieved from electromyograms, nerve conduction studies, muscle biopsies, magnetic field imaging and biofluid analysis [3,4]. The search for ALS/MND biomarkers useful for diagnosis, prognosis and analysis of drug efficacy includes a variety of molecules found in biofluids and other techniques including: heavy and light chain neurofilaments, TAR DNA-binding protein 43 (TDP-43), a lipid peroxidation product (4-hydroxy-2,3-nonenal), a urinary neurotrophin receptor p75 extracellular domain, cystatin C, mRNA, miRNA, extracellular glutamate, markers

of inflammation, microglial activation, electrical impedance myography, rate of disease progression, spinal cord imaging and others [1,5–17]. Thus far, none of these biomarkers have been sufficiently validated to be incorporated into the clinical standard of care [1,3,9,15,18].

Biomarker exploration has increased in recent years due to advances in cellular biology. The discovery of intercellular communication through exosomes has initiated new avenues for biomarker exploration. Exosomes are characterized as lipid membrane vesicles of endosomal origin of 30–200 nm in size, that contain a heterogeneous mix of messenger RNA (mRNA), microRNA (miRNA), transfer RNA (tRNA), Y RNA, small non-coding RNA (sRNA), DNA, lipids and proteins [19]. Extracellular vesicles (EVs) are a more inclusive term for nucleus-absent, lipid bilayer particles, including exosomes, that are naturally released from the cell [20]. EVs released into the extracellular matrix and taken up by adjacent cells impact cellular function of the recipient cells and possess both therapeutic and pathogenic potential [21]. EVs are thought to be expelled from all cell types and can be isolated from diverse biological fluids including cerebrospinal fluid (CSF), plasma, serum, breast milk, lymph, bile and saliva. EVs are remarkably stable in bodily fluids, providing protection for their molecular cargo from enzymatic breakdown. This stability combined with their availability in easily obtainable biological fluids make them of interest as potential reservoirs for disease biomarkers, which in turn could be useful for assessing the efficacy of therapeutic interventions [22]. Cancer research has demonstrated that changes in disease progression correlate with biological changes within EVs [23,24] and this has made EV analysis a particularly attractive option for biomarker research.

In parallel with current research on EVs, the investigation of miRNA has independently shown promise in the quest for biomarkers. Since miRNA are post-transcriptional regulators of gene expression, mediated via suppression of the translation of mRNAs or degradation of target mRNAs, they transmit executable instructions. They have been identified as potential biomarkers in many fields including cancer [25], AD [26], systemic lupus erythematosus [27], traumatic brain injury [28], cardiovascular disease [29], PD [30], multiple sclerosis [31] and diabetes [32]. Since miRNA are found as cargo within EVs and the lipid membrane surrounding EVs protects the miRNA from enzymatic degradation, there is good rationale for examining miRNA extracted from isolated EVs. Added to this the potential for selectively enriching EVs by subtypes based on the specific protein surface markers, these techniques can be targeted and potentially produce reliable, stable disease markers.

In this study, we have identified eight miRNA sequences from enriched EV extractions of blood plasma that consistently and significantly differentiate ALS/MND patients from healthy controls. Since the composition of blood extractions probably includes small molecules and some other EV subtypes, we choose here to use the more generic term of EV [20]. Exploiting cell-specific protein markers, we isolated a neural-enriched sub-population of extracellular vesicles (NEE) as a mechanism for analysing neural-specific cargo. This technique generates a pool of NEE that have the potential to be much more specific, reliable, and repeatable than other sources of biomarkers [33]. We compared the miRNA cargo from NEE in order to examine differential expression of miRNA between plasma samples from healthy controls

and ALS/MND patients. A complete replication of these biomarkers using identical techniques, but a second cohort of individuals supported the usefulness of miRNA fingerprints for further discovery.

## 2. Methods

### 2.1. Clinical samples

Forty total plasma samples were analysed in two independent experiments performed using identical criteria. Ten plasma samples were obtained from a blood draw of 10 ALS/MND patients at the time they enrolled in a Phase IIa human clinical trial (NCT03580616). ALS/MND patients were compared with 10 healthy control plasma samples (Innovative Research Inc., Novi, MI, USA). Following this experiment, a second cohort of 10 ALS/MND patients and 10 controls were independently analysed using the same methods and the results compared for repeatability. ALS/MND patients met the following criteria: (1) diagnosis of probable or definite ALS/MND based on the El Escorial criteria [34] within the last 3 years prior to study enrolment; (2) ALSFRS-R score > 25 and a FVC score  $\geq$  60% predicted; (3) age  $\geq$  18 years old. Prescription medications of both Riluzole and Enderavone/Radicava were allowed as long as the patient had taken these FDA-approved drugs for three months prior to trial enrolment and maintained a stable dose throughout the trial. None of the ALS/MND patients had a diagnosis or previous history of ischemic stroke, brain tumour, uncontrolled diabetes, renal insufficiency or severe hypertension. Severe hypertension (asymptomatic or hypertensive urgency) was defined as severely elevated blood pressure (180 mm Hg or more systolic, or 110 mm Hg or more diastolic) without acute target organ injury. None of the ALS/MND patients had a diagnosis or previous history of peripheral neuropathy or any other comorbid progressive neurodegenerative disease such as AD, PD, Lewy body disease, Pick's disease, Huntington's disease or progressive supranuclear palsy. None of the ALS/MND patients were undergoing any chemotherapy or radiation therapy for any cancer. None were pregnant women or women who were breast feeding a child. Genetic analysis was not performed on these patients as it was outside the scope of this study. In addition to the 20 control patients identified above, an additional four healthy control plasma samples were used in a pilot study to determine if there was sufficient material for RNA extraction, NGS and qPCR (Qiagen Genomic Services). The pilot study validation also compared miRNA content of different extraction fractions to examine them for distinct signatures.

### 2.2. Plasma extraction

Venous blood was drawn into K2 EDTA tubes followed by immediate centrifugation at 2000g for 15 min (4°C). The plasma was removed prior to being frozen at –80°C. Time between blood collection and freezing was less than 1 h.

### 2.3. EV extraction

Plasma samples were thawed on ice or at 4°C, treated with thrombin to remove fibrinogen, and the EVs were precipitated using polyethylene glycol (SBI ExoQuick, cat. no. EXOQ5TM-1, System Biosciences, Palo Alto, CA, USA). L1

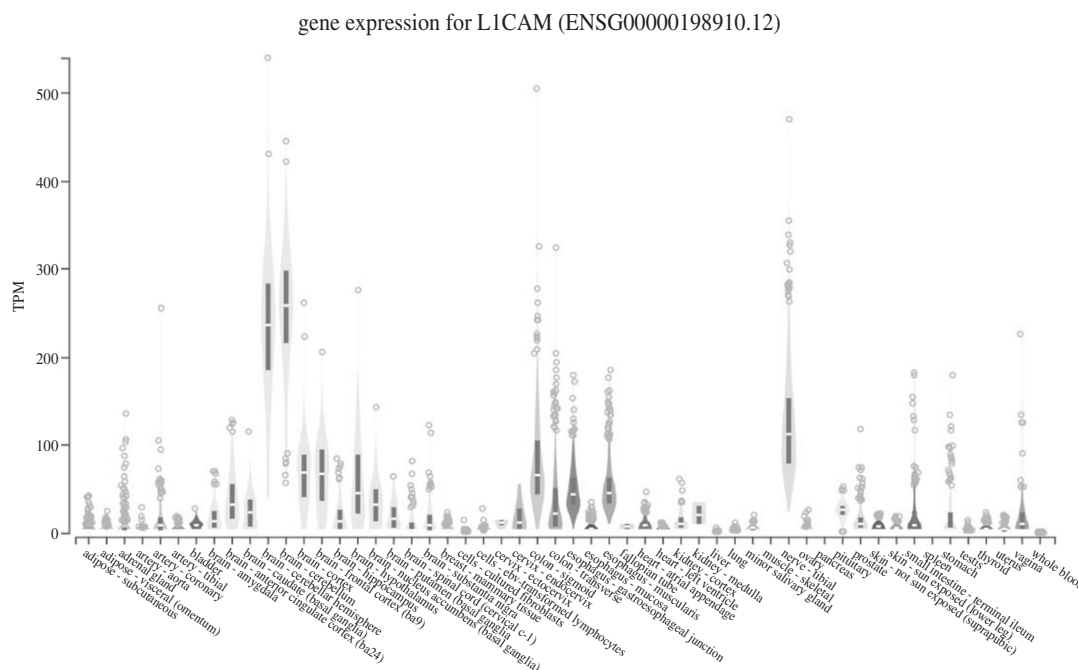


**Figure 1.** L1 cell adhesion molecule (L1CAM) expression is enriched in the brain. Expression values are shown in transcripts per million (TPM). Figure is from the Genotype-Tissue Expression (GTEx) Project which is supported by the Common Fund of the Office of the Director of the National Institutes of Health, and by NCI, NHGRI, NHLBI, NIDA, NIMH and NINDS (GTEx Portal Analysis Release V8, dbGaP Accession phs000424.v8.p2, accessed 22 January 2020, <https://gtexportal.org/home/gene/L1CAM>); see [35].

cell adhesion molecule (L1CAM) antibodies were used to selectively separate NEE [33]. Since L1CAM is a neural adhesion molecule and is highly expressed in brain and neural tissues (figure 1) [35], this step creates a neural-enriched fraction of EVs with characteristics consistent with exosomes. In brief, 500  $\mu$ l of plasma was incubated with 15  $\mu$ l thrombin at room temperature for 30 min. To this 485  $\mu$ l of sterile Dulbecco's phosphate-buffered saline balanced salt solution (DPBS calcium- and magnesium-free, Caisson Labs PBL01, Smithfield, UT, USA) mixed with three times the recommended concentrations of Halt protease inhibitor cocktail (cat. no. 78429, Thermo Fisher Scientific, Waltham, MA, USA) and Halt phosphatase inhibitor cocktail (cat. no. 78426, Thermo Fisher Scientific, Waltham, MA, USA) was added. The mixture was then centrifuged at 4500g for 20 min (4°C). To the supernatant, ExoQuick precipitation solution (252  $\mu$ l, cat. no. SBI EXOQ20A-1, System Biosciences Inc, Palo Alto, CA, USA) was then added to precipitate extracellular vesicles and the solution was incubated at 4°C for 1 h. The sample was centrifuged at 1500g for 20 min (4°C), and the supernatant discarded. The pellet was resuspended in 500  $\mu$ l of ultra-pure water that contained the 3 $\times$  protease and phosphatase inhibitors, vortexed gently and then placed on a rotating mixer overnight. This fraction represents the total extracellular vesicle extraction.

#### 2.4. Neural-enriched EV extraction

Enrichment of neural-enriched EVs was accomplished by the addition of 4  $\mu$ g of mouse anti-human CD171 (L1 cell adhesion molecule (L1CAM) neural adhesion protein) monoclonal antibody [cat. no. eBIO5G3 (5G3), (13-1719-82), Biotin, eBioscience™ Antibodies, Thermo Fisher Scientific, Waltham, MA, USA) in 50  $\mu$ l of 3% bovine serum albumin (BSA) (cat. no. 37525, Block BSA 10 $\times$  in PBS, Thermo Fisher Scientific, Waltham, MA, USA) for 60 min at 4°C on a rotating mixer.

To this solution, we then added 15  $\mu$ l of streptavidin-agarose resin (cat. no. 53116, Pierce Streptavidin Plus UltraLink Resin, Thermo Fisher Scientific, Waltham, MA, USA) plus 25  $\mu$ l of 3% BSA. This mixture was incubated at 4°C on a rotating mixer for 30 min followed by the addition of 4  $\mu$ l of ultra-pure 1 M TRIS-HCl pH 8.0 (cat. no. 15568025, Thermo Fisher Scientific, Waltham, MA, USA) to adjust pH to 7.0. The mixture was then centrifuged at 200g for 10 min (4°C). The supernatant fraction represents the total heterogeneous extracellular vesicle population minus the extracellular vesicles with L1CAM neural surface proteins, a fraction which we designate as T-N. The pellet containing the neural-enriched EVs (NEE) was then suspended in 200  $\mu$ l of 0.1 M glycine-HCl (pH 2.5) and the solution was strongly vortexed and centrifuged at 4500g for 5 min (4°C). The supernatant was recovered and neutralized with 15  $\mu$ l 1 M TRIS-HCl pH 8.0. The T-N and the NEE fractions were tested for protein content using Molecular Probes Quant iT Qubit Protein Assay Kit (cat. no. Q33211, Thermo Fisher Scientific, Waltham, MA, USA) using a Qubit 3 fluorometer (cat. no. Q33216, Invitrogen, Thermo Fisher Scientific, Waltham, MA, USA) and frozen in aliquots (–80°C).

#### 2.5. Characterization of extracellular vesicles

EVs were characterized using a ZetaView NTA System (Particle Metrix Inc. Henderson, NV, USA) in both light and fluorescence modes (cat. no. EXONTA110A-1, System Biosciences Inc., Palo Alto, CA, USA). Further characterization of surface proteins was conducted using the following kits according to manufacturer's instructions: human CD81 ELISA Kit (Sandwich ELISA) (cat. no. LS-F55938, LSBio Seattle, WA, USA); human CD63 ELISA Kit (Sandwich ELISA) (cat. no. LS-F7104, LSBio Seattle, WA, USA) and Exo-Check exosome antibody array (Neuro) (cat. no. EXORAY500A-8, System Biosciences Inc., Palo Alto, CA, USA).

## 2.6. RNA extraction from EVs, library construction and next-generation sequencing

RNA was isolated from purified NEE using the ExoRNeasy Serum/Plasma Kit (cat. no. 77023, Qiagen, Hilden, Germany) at Qiagen Genomic Services, Frederick, MD, USA. Briefly, 5  $\mu$ l total RNA was used to prepare the miRNA NGS libraries using the QIAseq miRNA Library Kit (cat. no. 331505, Qiagen, Hilden, Germany). RNA was ligated using adapters containing unique molecular indices (UMIs), and the RNA was converted to cDNA. Amplification of the cDNA was conducted using PCR (22 cycles) during which time PCR indices were added. Following purification, library preparation QC was conducted using a Bioanalyzer 2100 (Agilent Technologies, Santa Clara, CA, USA). Libraries were pooled in equimolar ratios based on quality of the inserts and the concentration measurements, quantified using qPCR, and sequenced on the NextSeq 500 System (Illumina, San Diego, CA, USA). FASTQ files were prepared and checked following de-multiplexing of raw data (bcl2fastq software, Illumina, San Diego, CA, USA; FastQC). For trimming, adapter and UMI information from raw reads was extracted using Cutadapt v. 1.11 [36]. Adapter sequences were removed and reads collapsed by UMI using a Qiagen in-house script. Reads were mapped using Bowtie2 v. 2.2.2 [37] where the criteria for aligning reads to spike-ins, abundant sequence and miRbase (v20) specified that the reads perfectly match reference sequences. EdgeR [38] was used to calculate differential expression and data normalized using trimmed mean of M-values (TMM) normalization [39]. miRNA was identified by mapping to miRBase (v. 20) [40]. The reliability of the identified miRNAs is noted to increase with the number of identified fragments expressed in tags per million (TPM) [39].

## 2.7. RNA extraction for qPCR quantitation of miRNA

Total RNA was extracted from the samples using ExoRNeasy Serum/Plasma Kit (cat. no. 77023, Qiagen, Hilden, Germany) high-throughput bead-based protocol using the QIAcube Connect (cat. no. 9002864, Qiagen, Hilden, Germany) at Qiagen Genomic Services. For miRNA quantitation, RNA was reverse transcribed to cDNA using the miRCURY locked nucleic acid (LNA) RT Kit (cat. no. 339340, Qiagen, Hilden, Germany). The RNA Spike-In Kit for RT (cat. no. 339390, Qiagen, Hilden, Germany) was applied to measure extraction efficiency and as quality control for RNA isolation and cDNA synthesis. Isolation controls were UniSp100 and UniSp101 in experiment 1 and UniSp2 and UniSp4 in experiment 2, and the cDNA synthesis controls for both experiments were UniSp3 and UniSp6. cDNA was diluted 50 $\times$  and assayed in 10  $\mu$ l qPCR reactions using the miRCURY LNA SYBR Green PCR kit (cat. no. 339345, Qiagen, Hilden, Germany; Qiagen Genomic Services, Frederick, Maryland, USA); each miRNA sequence (hsa, *Homo sapiens*) was assayed once by qPCR for miR-23a-3p, miR-30c-5p, miR-103a-3p, miR-191-5p, and miR-451a for experiment 1 and miR-103a-3p, miR-23a-3p, miR-30c-5p, miR-142-3p and miR-451a for experiment 2. miR-103a-3p, miR-23a-3p, and miR-30c-5p are known to be expressed in a majority of sample types at a consistent concentration, and therefore were used to evaluate miRNA content of samples. To assess any contribution to miRNA signal from haemolysis in plasma samples, the ratio of the differential

expression of miR-451a (highly expressed in thrombocytes) with miR-23a-3p (which has relatively stable expression in serum and is not affected by haemolysis), was determined. A ratio greater than 7.0 indicates an increased risk of haemolysis. Negative controls excluding template from the reverse transcription reaction was performed and profiled in the same manner as the samples and spike-ins.

## 2.8. cDNA qPCR

qPCR of cDNA generated from miRNA was conducted in accordance with MIQE guidelines [41] at Qiagen Genomic Services. The relative quantitation of 34 target miRNAs selected from the NGS results was determined by qPCR using SYBR Green detection on a LightCycler<sup>®</sup> 480 Real-Time PCR System (Roche, Basel, Switzerland) in 384 well plates. A positive reaction is detected by accumulation of a fluorescent signal. The cycle threshold (Ct) is defined as the number of cycles required for the fluorescent signal to cross the threshold (i.e. exceed background levels). The amplification curves were analysed using Qiagen software (v. 1.5.1.62 SP3), both for determination of Ct and for specificity, according to melt curve analysis.

## 2.9. Data analysis

The most stably expressed genes were selected as house-keeping genes by NormFinder [42] and a geometric mean was calculated using the top 3 (miR-29b-3p, miR-126-5p and miR-146a-5p). Consideration to use additional house-keeping genes was evaluated following a stepwise inclusion protocol comparing the pairwise variation ( $V_n/n+1$ ) calculated between two sequential normalization factors [43]. Since the pairwise variation of  $V_3/4$  was below 0.05, we did not include a fourth house-keeping gene. All cycle-time expression values were, therefore, normalized to the geometric mean of the three most stable genes and standard equations were used to calculate  $\Delta$ Ct,  $\Delta\Delta$ Ct and  $2^{-(\Delta\Delta$ Ct)}.

## 2.10. Statistical analysis

Differential expression analysis of the miRNA identified through NGS was performed using EdgeR [38] at Qiagen Genomic services. For normalization, the trimmed mean of M-values method based on log-fold and absolute gene-wise changes in expression levels between samples (TMM normalization) was used. Differential expression analysis was estimated by an exact test assuming a negative binomial distribution step ( $p < 0.05$  was determined as statistically significant).

We compared the gene fold expression [ $2^{-(\Delta\Delta$ Ct)}] median scores for ALS/MND patients and controls in each of the two replicated experiments. Plots of the data distributions did not conform to normal distributions, so we used non-parametric analysis, specifically a two-tailed Mann-Whitney *U* Test, to examine two alternative hypotheses for each of the 34 miRNA sequences of interest:

- H<sub>0</sub>: the miRNA sequences were drawn from the same population, e.g. median values of  $2^{-(\Delta\Delta$ Ct)} of the miRNA sequence are the same for ALS/MND patients and controls;
- H<sub>1</sub>: The miRNA sequences were drawn from different populations, e.g. median values of  $2^{-(\Delta\Delta$ Ct)} of the miRNA

**Table 1.** Differentially expressed miRNA as determined by qPCR of plasma samples comparing a total of 20 ALS patients and 20 controls reported from two identical, independent experiments (designated 1 and 2) using a different cohort of individuals in each experiment. Statistics were performed using a two-tailed Mann–Whitney *U*-test. Median values refer to fold gene expression  $2^{-(\Delta\Delta Ct)}$ . Fold regulation was reported in a biologically relevant way and is defined as, fold change in cases where fold change is greater than one, and in cases where fold change is less than one, fold regulation equals negative one divided by fold change. Direction of fold regulation indicates differential expression between ALS patients compared to healthy controls where an upregulation indicates higher median expression in ALS patients and downregulation indicates decreased expression.

experiment	miRNA ID	significance	Z-statistic	median control	median ALS	fold regulation	direction
1	miR-146a-5p	$p < 0.05$	-2.02	1.00	1.21	1.2	upregulated
2	miR-146a-5p	$p < 0.05$	-2.44	1.03	1.43	1.4	upregulated
1	miR-199a-3p	$p < 0.05$	-2.44	0.97	1.28	1.4	upregulated
2	miR-199a-3p	$p < 0.001$	-3.38	1.08	2.86	2.7	upregulated
1	miR-4454	$p < 0.05$	2.44	1.10	0.54	-1.7	downregulated
2	miR-4454	$p < 0.05$	2.44	0.97	0.44	-1.8	downregulated
1	miR-10b-5p	$p < 0.01$	2.61	1.00	0.58	-2.1	downregulated
2	miR-10b-5p	$p < 0.0001$	4.09	1.27	0.19	-7.0	downregulated
1	miR-29b-3p	$p < 0.001$	0.63	1.00	0.53	-1.7	downregulated
2	miR-29b-3p	$p < 0.01$	3.27	0.98	0.61	-1.7	downregulated
1	miR-151a-3p	$p < 0.01$	-2.88	0.97	1.49	1.5	upregulated
2	miR-151a-3p	$p < 0.01$	-2.98	1.22	2.62	2.2	upregulated
1	miR-151a-5p	$p < 0.001$	-3.83	1.07	1.38	1.4	upregulated
2	miR-151a-5p	$p < 0.001$	-3.59	1.04	3.92	3.2	upregulated
1	miR-199a-5p	$p < 0.001$	-3.49	1.14	1.91	1.9	upregulated
2	miR-199a-5p	$p < 0.001$	-3.59	1.10	5.16	4.2	upregulated

sequence are different for ALS/MND patients and controls; with the null hypothesis  $H_0$  being rejected at  $p < 0.05$ .

### 3. Results

In two separate experiments using a different cohort of patients and controls for each experiment, we found eight miRNA sequences that were significantly and consistently different between ALS/MND patients and healthy controls (table 1). Five miRNA sequences were upregulated in ALS/MND patients and three were downregulated (figure 2). The value and interpretation of these results is linked to the implementation of careful experimental quality controls which are reported below.

#### 3.1. EV characterization

The absolute purity of the NEE fraction used in this experiment was not known; therefore, we refer to our extraction in the larger sense of extracellular vesicles *sensu* Théry *et al.* [20]. Nevertheless, all indicators suggest that the miRNA expression reflect differences found within neural-enriched exosomes. The particles recovered from our extraction procedures were of an appropriate size and composition to be consistent with exosomes [20,44,45] with a median peak size of 102 nm for NEE (table 2). The tetraspanins CD81 and CD63 which are known to be enriched in many exosomes were abundant and concentrated in NEE (CD81: 5.2–8.7 billion  $\mu\text{l}^{-1}$ ,  $n = 20$ ; CD63: 7.4–13.7 billion  $\mu\text{l}^{-1}$ ,  $n = 6$ ). We also note that tumour susceptibility gene 101 (TSG101), a component of the endosomal sorting complexes required

for transport (ESCRT-I) complex, which is common in exosomes, was present and that a marker of cell contamination, calnexin, was absent. In the NEE fraction, we also found the presence of neural markers including: L1 transmembrane, neural cell adhesion, total tau, glutamate receptor 1 and proteolipid proteins (figure 3).

#### 3.2. Next generation sequence pilot study

The NGS pilot analysis was conducted to examine the quality and quantity of RNA within the NEE fraction, and to determine if the isolated NEE fraction differed from the T-N EV fraction in miRNA content. We successfully prepared, quantified and sequenced miRNA NGS libraries for all samples. The data passed all QC metrics; the NGS data had a high Q-Score (greater than 30), indicating good technical performance of the NGS experiment. An average of 4.6 million unique molecular index (UMI)-corrected reads per sample were obtained and the average percentage of mapable reads was 32.0%. We identified 256 miRNAs with  $\geq 1$  tags-per-million mapped reads (TPM) and 149 with  $\geq 10$  TPMs. Results comparing UMI corrected reads (3.8 million: 5.3 million), miRNA/smallRNA (6.6%:4.7%) and mapped genome (23.9%:23.8%) did not reveal notable differences between the two groups T-N and NEE, respectively ( $n = 4$  for each category). NormFinder analysis returned 25 stably expressed miRNAs, including the constitutively expressed miR-103a-3p with abundance measures between 294 and 3966 average TPM. Comparison between T-N and NEE identified 39 differentially expressed miRNA ( $p$ -values  $< 0.05$ ), within this small NGS pilot study.

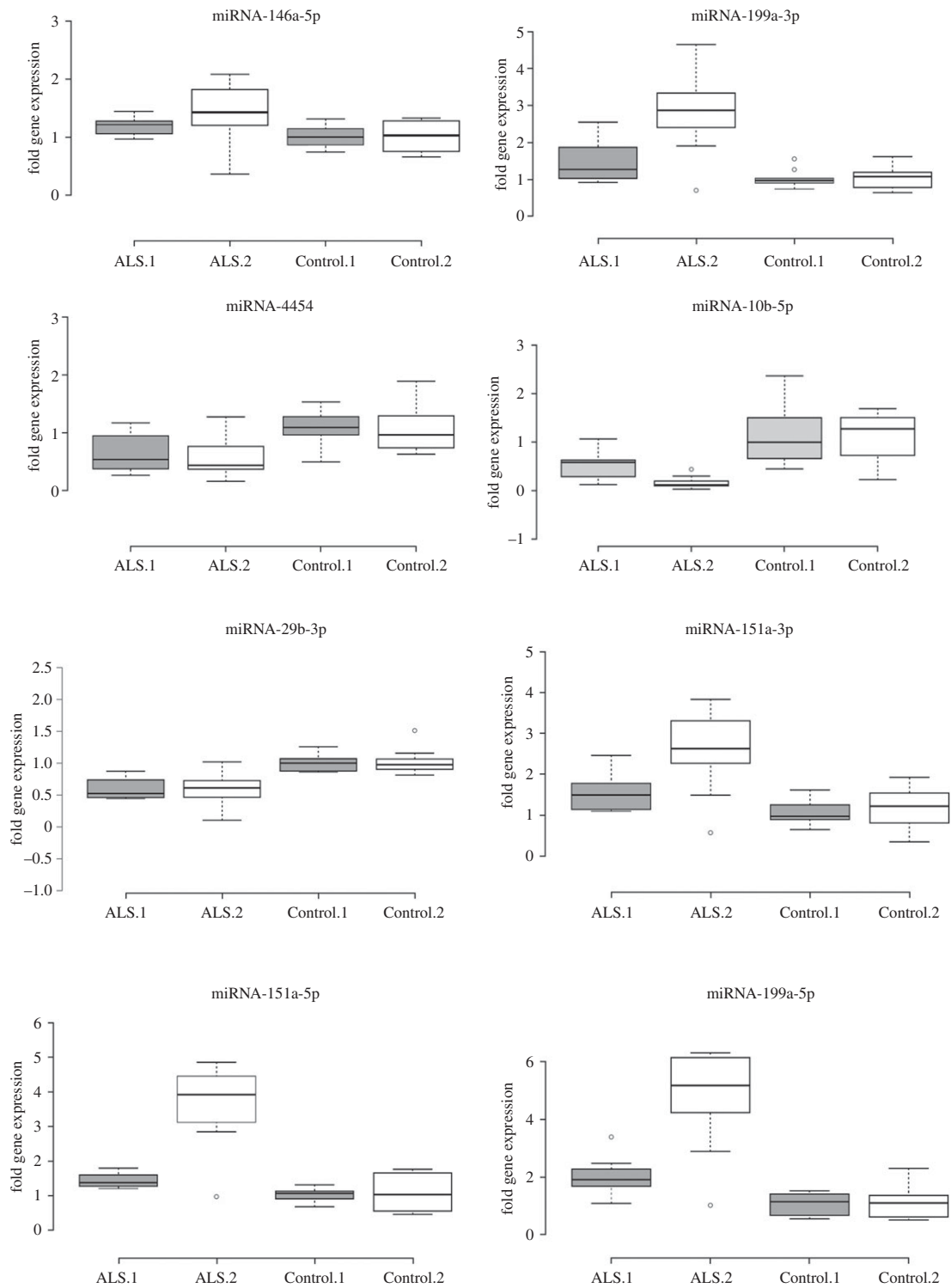


**Figure 2.** Box-plot representation of variability in gene fold expression [ $2^{-(\Delta\Delta Ct)}$ ] in eight miRNA comparing ALS patient and healthy controls in each of two replicated experiments comprised of separate individual cohorts. All eight miRNA differed statistically between patients and controls in each of the analysed cohort experimental groups. A two-tailed Mann–Whitney *U* Test (non-parametric based on the fact that data distribution plots did not conform to normal distributions) identified statistical differences ( $p < 0.05$ ). ALS.1 and Control.1 (shaded box) represent the first experiment with  $n = 10$  samples in each group. ALS.2 and Control.2 (open box) represent an independent replication using a new cohort of patients and controls each with  $n = 10$  samples. Center lines show the medians; box limits indicate the 25th and 75th percentiles; whiskers extend 1.5 times the interquartile range from the 25th and 75th percentiles, outliers are represented by circles.

### 3.3. NGS analysis of ALS/MND patient and control plasma using NEE

Next generation sequencing analysis identified miRNA, small RNA, genome-mapped, out-mapped, high-abundance RNA and unmapped reads, the latter of which did not align to the genome. We characterized miRNA as having 18–23 nucleotide lengths. The average number of UMI-corrected

reads per sample was 6.6 million, with an average percentage of mappable reads of 61.5%, indicating usable data.

### 3.4. Expression levels of miRNA

A total of 350 miRNAs were identified with a call rate  $\geq 1$  TPM and 219 were found to have a call rate  $\geq 10$  TPM. Statistical analysis of NGS data from extracellular vesicles

**Table 2.** Characterization of extracellular vesicles using nanoparticle tracking analysis suggests that vesicles are intact and parameters are consistent with exosomes. Median values reported for dominant peak.

	neural-enriched EV		total EV	
	fluorescence	scatter	fluorescence	scatter
	<i>n</i> = 3	<i>n</i> = 3	<i>n</i> = 4	<i>n</i> = 4
particle diameter	102 nm	126 nm	142 nm	130 nm
full-width half-max	95 nm	98 nm	101 nm	106 nm
representation	85%	100%	94%	97%
span (90x–10x)/50x	1.6	1	1.1	1.2

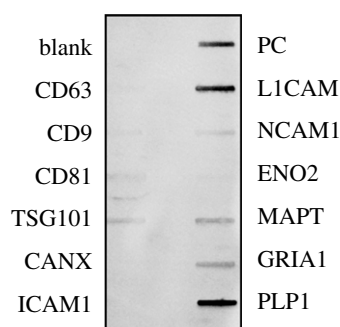


**Figure 3.** Exosome antibody detection of proteins found in neural-enriched exosome (NEE) extracts: Blank is negative control; CD63, CD9, CD81 are tetraspanins (CD63 and CD81 were confirmed independently through ELISAs); TSG101 is a component of the ESCRT-I complex; CANX is a calnexin cell contamination marker; ICAM1 is an intercellular adhesion molecule; PC is a positive control for HRP detection; and neural marker proteins include L1 transmembrane (L1CAM), neural cell adhesion 1 (NCAM1), enolase 2 (ENO2), total tau (MAPT), glutamate receptor 1 (GRIA1) and proteolipid 1 (PLP1).

(NEE) extracted from the plasma of 10 healthy control and 10 ALS/MND patients returned 101 significantly differentially expressed miRNA ( $p < 0.05$ ). From these 101 miRNA, 34 were chosen for relative-quantification using qPCR.

### 3.5. qPCR quantitation; miRNA QC results

We observed a steady level of expression of UniSp3 and UniSp6 in every sample indicating the RT and qPCR reactions were successful. Similar Cts for all negative controls indicate none of the samples contained inhibitors. One sample had a slightly elevated haemolysis ratio (greater than 7.0), which we determined to be insufficient to exclude from further analysis. We report Cts between 20 and 30 within all 40 samples, indicating there was enough miRNA to proceed with the downstream experiments.

### 3.6. qPCR quantitation of differentially expressed miRNA

From the 101 species of miRNA identified as differentially expressed by NGS, we selected 34 for downstream qPCR quantitation. The criteria for selection were based on (1) miRNA that were significantly differentially expressed between the controls and the patients, as determined by

NGS, and; (2) miRNA that were detected in the NGS and had previously been identified in the literature as being of interest in neurodegenerative disease.

Statistical analysis of the 34 target miRNA sequences from  $n = 10$  controls and  $n = 10$  patients returned highly significant comparative data, suggesting robust results. Thus, we repeated the entire experiment using identical methods but using a new cohort of patient and control samples. Statistical analysis of the replicate experiments returned eight miRNA that were differentially expressed between NEE derived from ALS/MND patients in comparison with a healthy control population of equal size in both experiment one and two (table 1). The following miRNA were analysed by qPCR but were found to be not significantly different between ALS/MND patients and controls, or not significantly different in one of the two experiments conducted using different patient cohorts which makes them not sensitive enough for use as ALS/MND biomarkers: let-7b-5p, let-7d-3p, let-7d-5p, miR-126-3p, miR-126-5p, miR-133a-3p, miR-1-3p, miR-143-3p, miR-146a-3p, miR-194-3p, miR-23a-3p, miR-330-3p, miR-338-3p, miR-339-3p, miR-339-5p, miR-451a, miR-517a-3p, miR-584-5p, miR-625-3p, miR-708-5p and miR-744-5p.

## 4. Discussion

We identified eight miRNA sequences derived from NEE extractions that consistently and significantly differentiate ALS/MND patients from healthy controls with a single blood draw. These miRNA sequences were drawn from two experiments using different patient and control cohorts each producing the same eight miRNA sequences. We suggest that these miRNA sequences, singly or in combinations, can confirm the diagnosis of ALS/MND based on standard clinical criteria and may allow ALS/MND to be diagnosed in pre-symptomatic individuals, rapidly speeding diagnosis and treatment. Furthermore, the upregulation or downregulation of these miRNA sequences may potentially allow the effectiveness of existing or novel treatments of ALS/MND to be rapidly assessed before any clinical changes in patient disease progression or symptoms.

EVs drawn from blood plasma are important reservoirs for biomarkers for three reasons: (1) they are stable and abundant in biological fluids; (2) blood plasma is routinely drawn from patients and this procedure is relatively non-invasive when compared with lumbar punctures or tissue biopsies; and (3) the cargo of EVs contain important biomolecules including

nucleic acids and proteins. Owing to unique proteins on the surface of EVs, subpopulations of specific origins can be enriched. For example, the presence of L1CAM was used in our experiments to isolate a sub-population of neural-enriched EVs. Although L1CAM is not exclusively expressed in the brain, the enrichment process enhances the chance that the biomarkers found are related specifically to neurodegeneration. The consistency of the results across two independent experiments achieved in this report supports this method as being robust and useful in the discovery of biomarkers. We examine only miRNA in this study, but it may be possible to use the same extraction and enrichment techniques to examine proteins, lipids, and other RNA species for biomarker potential.

Katsu *et al.* [46], in a study with five ALS patients and five control patients using extraction methods similar to ours, identified 30 miRNA that differed between the two groups but these were not verified by qPCR. This contrasts with our study that had a larger sample size (20 per independent experiment  $\times$  2 experiments = 40 total individual samples) and was validated by qPCR. Data from our NGS experiment, which helped to identify miRNA sequences of interest for the more rigorous qPCR analysis, revealed only two overlapping miRNA sequences (miR-24-3p, miR-150-3p) with Katsu *et al.* [46] neither of which we chose for further study. Katsu *et al.* [46] suggested that the data they presented should be validated by qPCR and that larger patient cohorts are needed to determine the broader application of the identified miRNA to ALS. The majority of the miRNA found by Katsu *et al.* [46] were not identified in our NGS study indicating that they were either not present in the samples we examined, or that their abundance was sufficiently low as to not be recognized. Of the two miRNA that did overlap between our NGS study and the Katsu *et al.* [46] study, we evaluated both after the necessary statistical adjustment for false discovery rates (FDR) and found that miR-24-3p was not significant between ALS/MND patients and controls (FDR  $p$ -value = 0.053), but that miR-150-3p was significant between ALS/MND patients and controls (FDR  $p$ -value = 0.006). These two miRNA that we identified in NGS have not undergone qPCR evaluation, therefore we cannot determine the importance of these miRNA as possible ALS biomarkers. We chose not to report the other possible 67 identified miRNA from our NGS analysis until they can be further analysed in a more quantitative fashion.

Numerous miRNA have been considered as potentially valuable for ALS/MND patient biomarker investigation by other researchers using CSF, peripheral blood leucocytes, muscle tissue or plasma/serum in the absence of extracellular vesicle isolation [47–60]. It is difficult to parse the comparable value of miRNA from different biological fluids and different methods of extraction and analysis. We do note that of those miRNA identified in other studies and which were included in our list of qPCR interrogated miRNA, the following did not meet the criteria to reject a hypothesis of similar expression values between ALS/MND patients and healthy controls in our sample population: let-7b-5p, let-7d-3p, let-7d-5p, miR-126-5p, miR-133a-3p, miR-143-3p, miR-146a-3p, miR-23a-3p, miR-338-3p, miR-451a, miR-584a-5p [49–53,56,60]. miR-146a-5p, miR-151a-5p, miR-199a-3p, miR-199a-5p were consistently significant in our analysis and found in other biofluids and fractions in other studies as important [51,60]. Of great interest is the associations of miR-151a-5p, miR-199a-3p, miR-199a-5p found by Raheja *et al.* [51] from circulating blood serum to be correlated with clinical ALS parameters in

a longitudinal analysis. In addition, Raheja *et al.* [51] found that miR-199a-5p was upregulated in both ALS and AD but that the expression levels could distinguish between ALS and AD patients. The expression of miR-146a-5p in CSF was downregulated in a sequencing study by Waller *et al.* [60] but they were unable to verify this result using qPCR. In our study, miR-146a-5p was analysed by qPCR and shown to be upregulated in NEE of two separate experiments using a different cohort of patients. We did not choose all the significant miRNA sequences identified in the NGS evaluation for qPCR and we are not reporting the full results of the NGS analysis because we recognize that individual miRNA should be fully evaluated using a more quantitative approach in order to understand their biological relevancy. We suggest that the extraction protocol followed in this study, extracting extracellular vesicles from blood plasma followed by enrichment of neural vesicles using L1CAM, leads to a more relevant pool of miRNA that is directly associated with neurodegenerative processes, is repeatable, and might be specifically useful as biomarkers for ALS/MND. The replication reported here using different cohorts of patients and controls supports this assertion. Ultimately, biomarkers for ALS/MND clinical diagnosis and prognosis may involve several combined approaches currently under investigation by multiple researchers. The precise disease related associations between the identified miRNA in our study and their biological targets, in the context of ALS/MND, are not yet fully known. We can draw important comparisons from studies of neurodegeneration in general.

miR-146a-5p is known to be involved in both influencing synaptic plasticity [61] and regulating the inflammatory response [62]. We report that miR-146a-5p was upregulated in the NEE of ALS/MND patient samples versus controls. Downregulation of miR-146a-5p leads to an increase in dendritic microtubule-associated protein 1B (MAP1B) translation which can reduce synaptic transmission in neurons and this pathway is part of the pathogenesis of Rett syndrome [63]. In this model, the decrease in miR-146a-5p resulted in an increase in MAP1B and corresponding AMPA receptor endocytosis. In the context of ALS/MND, upregulation of miR-146a-5p could negatively impact synaptic plasticity [61]. Similarly, miR-146a-5p may play a role in spinal muscular atrophy (SMA) as evidenced by reduced SMA astrocyte-induced motor neuron loss when miR-146a-5p is inhibited [64]. Taken together, these data suggest that an increase in miR-146a-5p, as seen in the current study, could trigger motor neuron loss which further supports the possible role of miR-146a-5p in the pathogenicity of ALS/MND.

The precise function of miR-146a-5p in ALS, however, could also be related to a role in anti-inflammation particularly within astrocytes [65–67]. Upregulation of miR-146a-5p in ALS/MND is consistent with Lu *et al.*'s [65] data suggesting that it binds to the 3' UTR of TRAF6 mRNA inhibiting both mRNA and protein expression of TRAF6 resulting in a reduction of neuropathic pain. miR-146a-5p seems to be correlated with neurodegeneration in general as it has been implicated in AD where it is also upregulated in superior temporal lobe neocortex which was found to be correlated with an increase in severity of disease with direct impact on immune response and inflammation [68]. We note that miR-146a has been found to be upregulated in AD brain tissues and downregulated in plasma, serum, and CSF of Alzheimer's patients [68–73]. miR-146a was not found to be upregulated in

four ALS, four PD or five schizophrenia temporal lobe neocortex tissues when compared with six control tissues [70].

Using a proprietary method of total exosome extraction (synthetic peptides, Venceremin) with a high affinity for heat shock proteins [74], Saucier *et al.* [75] found two miRNA related to ALS patients which differed from controls and which overlap with our own miRNA analysis of NEE. In the case of miR-199a-3p, they note this miRNA was downregulated in their analysis of total exosomes, while we found that it was consistently upregulated when examining the specific subpopulation of NEE. However, both our studies note miR-4454 as upregulated in ALS/MND patients when compared to control patient samples.

miR-199a is highly expressed in rat neural tissues [76]. miR199a-3p regulates the expression of mammalian target of rapamycin protein (mTOR) which plays a role in protein synthesis, cell growth, and is an important protein for axon regeneration and plasticity following central nervous system damage [77]. When upregulated, miR199a-3p should decrease the mTOR protein with a predicted negative effect on regeneration processes for damaged neurons. This miRNA sequence could be an important indicator for ALS/MND.

miR-10b-5p has been implicated in Huntington's disease pathogenicity where it was found to be upregulated in post-mortem prefrontal cortex tissue [78]. We note that miR-10b-5p was consistently downregulated in ALS/MND patients in this study. Since the presence of miR-10b-5p has been shown to suppress brain-derived neurotrophic factor (BDNF) [79], the downregulation of miR-10b-5p would be expected to increase BDNF. This result could have positive effects on memory and learning, synaptogenesis, and survival and differentiation of striatal neurons, and is consistent with an increase in BDNF found in the lymphocytes of ALS patients [80–82].

Although miR-29 sequences are well known to have anti-tumour effects, they also regulate genes related to proapoptotic/antiapoptotic pathways [83]. More research is needed to understand the role this miRNA might play in ALS/MND pathogenesis or the cellular response to disease symptoms in ALS/MND.

miR-151a-3p has previously been linked with autism and schizophrenia (miR-151), however, the fold regulation is reversed in our study of ALS/MND, being upregulated here and downregulated in these two other diseases using

different sample types [84,85]. However, we note that miR-151a-3p is also upregulated in AD (noted in circulating RNA isolated directly from blood [86]) and in PD (reported from CSF exosomes [87]) but not from neural-enriched EVs as found in our study.

miR-151a-5p is thought to participate in the maintenance of cell viability through changing the cell response to oxidative stress [88]. Since the familial ALS gene mutation SOD-1 relates to an increase in mitochondrial reactive oxygen species and subsequent vulnerability to excitotoxicity [89], it is plausible that miR-151a-5p plays a role in ALS/MND.

Lastly, the upregulation miR-199a-5p, which is seen in this study, has been demonstrated to have protective effects in rat spinal cord injury models [90]. We suggest that this miRNA has similar protective effects in ALS/MND motor neuron degeneration.

## 5. Conclusion

We successfully extracted and characterized a neural-enriched subpopulation of EVs from 40 ALS/MND patient and control samples and determined that they contain sufficient miRNA to conduct NGS and qPCR. In repeated experiments using different patient and control cohorts, we have identified eight miRNA sequences that are differentially expressed in ALS/MND patients and healthy controls. This replication provides strong evidence that these miRNA sequences individually or in combination should be further investigated as ALS/MND biomarkers using larger sample sizes. Further work to compare these results with other neurodegenerative conditions is also warranted.

**Ethics.** This study was approved by the institutional ethical review board of Dartmouth Hitchcock Medical School under the FDA approved Phase IIa human clinical trial (NCT03580616) and by Innovative Research FDA Approval (3003372368). All samples were collected following written informed consent.

**Competing interests.** The Brain Chemistry Labs is filing a patent on the use of this biomarker.

**Funding.** This work was supported by Brian & Wetonnah McCoy, The Lee's Cares Foundation, The Nicholas Martin Jr. Family Foundation, The One Foundation and The Satter Foundation.

**Acknowledgements.** We thank V. Portnoy for partial Zetaview analysis, E. Stommel, Principal Investigator of the Phase IIa ALS trial at Dartmouth Medical School for ALS patient plasma samples.

## References

- Hosaka T, Yamashita T, Tamaoka A, Kwak S. 2019 Extracellular RNAs as biomarkers of sporadic amyotrophic lateral sclerosis and other neurodegenerative diseases. *Int. J. Mol. Sci.* **20**, 3148. (doi:10.3390/ijms20133148)
- Levine TD *et al.* 2017 Phase I clinical trial of safety of L-serine for ALS patients. *Amyotroph. Lateral Scler. Front. Degener.* **18**, 107–111. (doi:10.1080/21678421.2016.1221971)
- Pasinetti GM *et al.* 2006 Identification of potential CSF biomarkers in ALS. *Neurology* **66**, 1218–1222. (doi:10.1212/01.wnl.0000203129.82104.07)
- Mayo Clinic. 2019 Amyotrophic lateral sclerosis (ALS): diagnosis and treatment. See <https://www.mayoclinic.org/diseases-conditions/amyotrophic-lateral-sclerosis/diagnosis-treatment/drc-20354027> (accessed on 27 April 2020).
- Ferrarese C *et al.* 2001 Decreased platelet glutamate uptake in patients with amyotrophic lateral sclerosis. *Neurology* **56**, 270–272. (doi:10.1212/WNL.56.2.270)
- Lu CH *et al.* 2015 Plasma neurofilament heavy chain levels and disease progression in amyotrophic lateral sclerosis: Insights from a longitudinal study. *J. Neurol. Neurosurg. Psychiatry* **86**, 565–573. (doi:10.1136/jnnp-2014-307672)
- Labra J, Menon P, Byth K, Morrison S, Vucic S. 2016 Rate of disease progression: a prognostic biomarker in ALS. *J. Neurol. Neurosurg. Psychiatry* **87**, 628–632. (doi:10.1136/jnnp-2015-310998)
- Shepherd SR, Wu J, Cardoso M, Wiklendt L, Dinning PG, Chataway T, Schultz D, Benatar M, Rogers ML. 2017 Urinary p75ECD: a prognostic, disease progression, and pharmacodynamic biomarker in ALS. *Neurology* **88**, 1137–1143. (doi:10.1212/WNL.0000000000003741)
- Poesen K, Van Damme P. 2019 Diagnostic and prognostic performance of neurofilaments in ALS. *Front. Neurol.* **9**, 1167. (doi:10.3389/fneur.2018.01167)
- Simpson EP, Henry YK, Henkel JS, Smith RG, Appel SH. 2004 Increased lipid peroxidation in sera of ALS patients: a potential biomarker of disease burden.

- Neurology* **62**, 1758–1765. (doi:10.1212/WNL.62.10.1758)
11. Boylan K, Yang C, Crook J, Overstreet K, Heckman M, Wang Y, Borchelt D, Shaw G. 2009 Immunoreactivity of the phosphorylated axonal neurofilament H subunit (pNF-H) in blood of ALS model rodents and ALS patients: evaluation of blood pNF-H as a potential ALS biomarker. *J. Neurochem.* **111**, 1182–1191. (doi:10.1111/j.1471-4159.2009.06386.x)
  12. Wilson ME, Boumaza I, Lacomis D, Bowser R. 2010 Cystatin C: a candidate biomarker for amyotrophic lateral sclerosis. *PLoS ONE* **5**, e15133. (doi:10.1371/journal.pone.0015133)
  13. Bede P, Bokde ALW, Byrne S, Elamin M, Fagan AJ, Hardiman O. 2012 Spinal cord markers in ALS: diagnostic and biomarker considerations. *Amyotroph. Lateral Scler.* **13**, 407–415. (doi:10.3109/17482968.2011.649760)
  14. Rutkove SB *et al.* 2012 Electrical impedance myography as a biomarker to assess ALS progression. *Amyotroph. Lateral Scler.* **13**, 439–445. (doi:10.3109/17482968.2012.688837)
  15. Tarasiuk J, Kułakowska A, Drozdowski W, Kornhuber J, Lewczuk P. 2012 CSF markers in amyotrophic lateral sclerosis. *J. Neural Transm.* **119**, 747–757. (doi:10.1007/s00702-012-0806-y)
  16. Feneberg E, Steinacker P, Lehnert S, Schneider A, Walther P, Thal DR, Linsenmeier M, Ludolph AC, Otto M. 2014 Limited role of free TDP-43 as a diagnostic tool in neurodegenerative diseases. *Amyotroph. Lateral Scler. Front. Degener.* **15**, 351–356. (doi:10.3109/21678421.2014.905606)
  17. Lu CH *et al.* 2015 Neurofilament light chain: a prognostic biomarker in amyotrophic lateral sclerosis. *Neurology* **84**, 2247–2257. (doi:10.1212/WNL.0000000000001642)
  18. von Neuhoff N *et al.* 2012 Monitoring CSF proteome alterations in amyotrophic lateral sclerosis: obstacles and perspectives in translating a novel marker panel to the clinic. *PLoS ONE* **7**, e44401. (doi:10.1371/journal.pone.0044401)
  19. Pegtel DM, Gould SJ. 2019 Exosomes. *Annu. Rev. Biochem.* **88**, 487–514. (doi:10.1146/annurev-biochem-013118-111902)
  20. Théry C *et al.* 2018 Minimal information for studies of extracellular vesicles 2018 (MISEV2018): a position statement of the International Society for Extracellular Vesicles and update of the MISEV2014 guidelines. *J. Extracell. Vesicles* **7**, 1535750. (doi:10.1080/20013078.2018.1535750)
  21. Cheruiyot C, Pataki Z, Ramratnam B, Li M. 2018 Proteomic analysis of exosomes and its application in HIV-1 infection. *Proteomics Clin. Appl.* **12**, 1700142. (doi:10.1002/prca.201700142)
  22. Manna I *et al.* 2018 Exosome-associated miRNA profile as a prognostic tool for therapy response monitoring in multiple sclerosis patients. *FASEB J.* **32**, 4241–4246. (doi:10.1096/fj.201701533R)
  23. Meng Y, Sun J, Wang X, Hu T, Ma Y, Kong C, Piao H, Yu T, Zhang G. 2019 Exosomes: a promising avenue for the diagnosis of breast cancer. *Technol. Cancer Res. Treat.* **18**, 1533033818821421. (doi:10.1177/1533033818821421)
  24. Shi M, Jiang Y, Yang L, Yan S, Wang Y-G, Lu X-J. 2018 Decreased levels of serum exosomal miR-638 predict poor prognosis in hepatocellular carcinoma. *J. Cell. Biochem.* **119**, 4711–4716. (doi:10.1002/jcb.26650)
  25. Chen B, Xia Z, Deng YN, Yang Y, Zhang P, Zhu H, Xu N, Liang S. 2019 Emerging microRNA biomarkers for colorectal cancer diagnosis and prognosis. *Open Biol.* **9**, 180212. (doi:10.1098/rsob.180212)
  26. Wu HZY, Ong KL, Seehar K, Armstrong NJ, Thalamuthu A, Brodaty H, Sachdev P, Mather K. 2015 Circulating microRNAs as biomarkers of Alzheimer's disease: a systematic review. *J. Alzheimer's Dis.* **49**, 755–766. (doi:10.3233/JAD-150619)
  27. Zheng X, Zhang Y, Yue P, Liu L, Wang C, Zhou K, Hua Y, Wu G, Li Y. 2019 Diagnostic significance of circulating miRNAs in systemic lupus erythematosus. *PLoS ONE* **14**, e0217523. (doi:10.1371/journal.pone.0217523)
  28. Atif H, Hicks SD. 2019 A review of MicroRNA biomarkers in traumatic brain injury. *J. Exp. Neurosci.* **13**, 117906951983228. (doi:10.1177/1179069519832286)
  29. Zhou SS, Jin JP, Wang JQ, Zhang ZG, Freedman JH, Zheng Y, Cai L. 2018 MiRNAs in cardiovascular diseases: potential biomarkers, therapeutic targets and challenges review-article. *Acta Pharmacol. Sin.* **39**, 1073–1084. (doi:10.1038/aps.2018.30)
  30. Roser AE, Caldi Gomes L, Schünemann J, Maass F, Lingor P. 2018 Circulating miRNAs as diagnostic biomarkers for Parkinson's disease. *Front. Neurosci.* **12**, 625. (doi:10.3389/fnins.2018.00625)
  31. Piket E, Zheleznyakova GY, Kular L, Jagodic M. 2019 Small non-coding RNAs as important players, biomarkers and therapeutic targets in multiple sclerosis: a comprehensive overview. *J. Autoimmun.* **101**, 17–25. (doi:10.1016/j.jaut.2019.04.002)
  32. Vaishya S, Sarwade RD, Seshadri V. 2018 MicroRNA, proteins, and metabolites as novel biomarkers for prediabetes, diabetes, and related complications. *Front. Endocrinol. (Lausanne)* **9**, 180. (doi:10.3389/fendo.2018.00180)
  33. Mustapic M, Eitan E, Werner JKI, Berkowitz ST, Lazaropoulos MP, Tran J, Goetzl EJ, Kapogiannis D. 2017 Plasma extracellular vesicles enriched for neuronal origin: a potential window into brain pathologic processes. *Front. Neurosci.* **11**, 278. (doi:10.3389/fnins.2017.00278)
  34. Brooks BR, Miller RG, Swash M, Munsat TL. 2000 El Escorial revisited: revised criteria for the diagnosis of amyotrophic lateral sclerosis. *Amyotroph. Lateral Scler.* **1**, 293–299. (doi:10.1080/146608200300079536)
  35. GTEx Portal. 2019 Gene expression for L1CAM. See <https://www.gtexportal.org/home/gene/ENSG00000198910> (accessed on 22 January 2020).
  36. Martin M. 2011 Cutadapt removes adapter sequences from high-throughput sequencing reads. *EMBnet.journal* **17**, 10. (doi:10.14806/ej.17.1.200)
  37. Langmead B, Salzberg SL. 2012 Fast gapped-read alignment with Bowtie 2. *Nat. Methods* **9**, 357–359. (doi:10.1038/nmeth.1923)
  38. Robinson MD, McCarthy DJ, Smyth GK. 2009 edgeR: a bioconductor package for differential expression analysis of digital gene expression data. *Bioinformatics* **26**, 139–140. (doi:10.1093/bioinformatics/btp616)
  39. Robinson MD, Oshlack A. 2010 A scaling normalization method for differential expression analysis of RNA-seq data. *Genome Biol.* **11**, R25. (doi:10.1186/gb-2010-11-3-r25)
  40. Kozomara A, Griffiths-Jones S. 2014 miRBase: annotating high confidence microRNAs using deep sequencing data. *Nucleic Acids Res.* **42**, D68–D73. (doi:10.1093/nar/gkt1181)
  41. Bustin SA *et al.* 2009 The MIQE guidelines: minimum information for publication of quantitative real-time PCR experiments. *Clin. Chem.* **55**, 611–622. (doi:10.1373/clinchem.2008.112797)
  42. Andersen CL, Jensen JL, Ørntoft TF. 2004 Normalization of real-time quantitative reverse transcription-PCR data: a model-based variance estimation approach to identify genes suited for normalization, applied to bladder and colon cancer data sets. *Cancer Res.* **64**, 5245–5250. (doi:10.1158/0008-5472.CAN-04-0496)
  43. Vandesompele J, De Preter K, Pattyn F, Poppe B, Van Roy N, De Paepe A, Speleman F. 2002 Accurate normalization of real-time quantitative RT-PCR data by geometric averaging of multiple internal control genes. *Genome Biol.* **3**, RESEARCH0034. (doi:10.1186/gb-2002-3-7-research0034)
  44. Witwer KW *et al.* 2013 Standardization of sample collection, isolation and analysis methods in extracellular vesicle research. *J. Extracell. Vesicles* **2**, 20360. (doi:10.3402/jev.v2i0.20360)
  45. Hill AF, Pegtel DM, Lambert U, Leonardi T, O'Driscoll L, Pluchino S, Ter-Ovanesyan D, Nolte-t Hoen ENM. 2013 ISEV position paper: extracellular vesicle RNA analysis and bioinformatics. *J. Extracell. Vesicles* **2**, 22859. (doi:10.3402/jev.v2i0.22859)
  46. Katsu M, Hama Y, Utsumi J, Takahina K, Yasumatsu H, Mori F, Wakabayashi K, Shoji M, Sasaki H. 2019 MicroRNA expression profiles of neuron-derived extracellular vesicles in plasma from patients with amyotrophic lateral sclerosis. *Neurosci. Lett.* **708**, 134176. (doi:10.1016/j.neulet.2019.03.048)
  47. Butovsky O *et al.* 2012 Modulating inflammatory monocytes with a unique microRNA gene signature ameliorates murine ALS. *J. Clin. Invest.* **122**, 3063–3087. (doi:10.1172/JCI62636)
  48. De Felice B, Guida M, Coppola C, De Mieri G, Cotrufo R. 2012 A miRNA signature in leukocytes from sporadic amyotrophic lateral sclerosis. *Gene* **508**, 35–40. (doi:10.1016/j.gene.2012.07.058)
  49. Waller R *et al.* 2017 Serum miRNAs miR-206, 143-3p and 374b-5p as potential biomarkers for amyotrophic lateral sclerosis (ALS). *Neurobiol. Aging* **55**, 123–131. (doi:10.1016/j.neurobiolaging.2017.03.027)
  50. Liguori M, Nuzziello N, Introna A, Consiglio A, Licciulli F, D'Errico E, Scarafino A, Distaso E, Simone

- IL. 2018 Dysregulation of microRNAs and target genes networks in peripheral blood of patients with sporadic amyotrophic lateral sclerosis. *Front. Mol. Neurosci.* **11**, 288. (doi:10.3389/fnmol.2018.00288)
51. Raheja R *et al.* 2018 Correlating serum micromRNAs and clinical parameters in amyotrophic lateral sclerosis. *Muscle Nerve* **58**, 261–269. (doi:10.1002/mus.26106)
52. Vrabec K, Boštjančič E, Koritnik B, Leonardiš L, Dolenc Grošelj L, Zidar J, Rogelj B, Glavač D, Ravnik-Glavač M. 2018 Differential expression of several miRNAs and the host genes AATK and DNM2 in leukocytes of sporadic ALS patients. *Front. Mol. Neurosci.* **11**, 106. (doi:10.3389/fnmol.2018.00106)
53. De Felice B *et al.* 2014 miR-338-3p is over-expressed in blood, CFS, serum and spinal cord from sporadic amyotrophic lateral sclerosis patients. *Neurogenetics* **15**, 243–253. (doi:10.1007/s10048-014-0420-2)
54. Toivonen JM, Manzano R, Oliván S, Zaragoza P, García-Redondo A, Osta R. 2014 MicroRNA-206: a potential circulating biomarker candidate for amyotrophic lateral sclerosis. *PLoS ONE* **9**, e89065. (doi:10.1371/journal.pone.0089065)
55. Takahashi I, Hama Y, Matsushima M, Hirotsani M, Kano T, Hohzen H, Yabe I, Utsumi J, Sasaki H. 2015 Identification of plasma microRNAs as a biomarker of sporadic amyotrophic lateral sclerosis. *Mol. Brain* **8**, 67. (doi:10.1186/s13041-015-0161-7)
56. Chen Y, Wei Q, Chen X, Li C, Cao B, Ou R, Hadano S, Shang H-F. 2016 Aberration of miRNAs expression in leukocytes from sporadic amyotrophic lateral sclerosis. *Front. Mol. Neurosci.* **9**, 69. (doi:10.3389/fnmol.2016.00069)
57. de Andrade HMT, de Albuquerque M, Avansini SH, de Rocha SC, Dogini DB, Nucci A, Carvalho B, Lopes-Cendes I. 2016 MicroRNAs-424 and 206 are potential prognostic markers in spinal onset amyotrophic lateral sclerosis. *J. Neurol. Sci.* **368**, 19–24. (doi:10.1016/j.jns.2016.06.046)
58. Tasca E, Pegoraro V, Merico A, Angelini C. 2016 Circulating microRNAs as biomarkers of muscle differentiation and atrophy in ALS. *Clin. Neuropathol.* **35**, 22–30. (doi:10.5414/NP300889)
59. Sheinerman KS *et al.* 2017 Circulating brain-enriched microRNAs as novel biomarkers for detection and differentiation of neurodegenerative diseases. *Alzheimer's Res. Ther.* **9**, 1–13. (doi:10.1186/s13195-017-0316-0)
60. Waller R, Wyles M, Heath PR, Kazoka M, Wollff H, Shaw PJ, Kirby J. 2018 Small RNA sequencing of sporadic amyotrophic lateral sclerosis cerebrospinal fluid reveals differentially expressed miRNAs related to neural and glial activity. *Front. Neurosci.* **11**, 731. (doi:10.3389/fnins.2017.00731)
61. Benoist M, Palenzuela R, Rozas C, Rojas P, Tortosa E, Morales B, González-Billault C, Ávila J, Esteban JA. 2013 MAP1B-dependent Rac activation is required for AMPA receptor endocytosis during long-term depression. *EMBO J.* **32**, 2287–2299. (doi:10.1038/emboj.2013.166)
62. Etzrodt M *et al.* 2012 Regulation of monocyte functional heterogeneity by miR-146a and Relb. *Cell Rep.* **1**, 317–324. (doi:10.1016/j.celrep.2012.02.009)
63. Chen YL, Shen CKJ. 2013 Modulation of mGluR-dependent MAP1B translation and AMPA receptor endocytosis by microRNA miR-146a-5p. *J. Neurosci.* **33**, 9013–9020. (doi:10.1523/JNEUROSCI.5210-12.2013)
64. Sison SL, Patitucci TN, Seminary ER, Villalon E, Lorson CL, Ebert AD. 2017 Astrocyte-produced miR-146a as a mediator of motor neuron loss in spinal muscular atrophy. *Hum. Mol. Genet.* **26**, 3409–3420. (doi:10.1093/hmg/ddx230)
65. Lu Y, Cao DL, Jiang BC, Yang T, Gao YJ. 2015 MicroRNA-146a-5p attenuates neuropathic pain via suppressing TRAF6 signaling in the spinal cord. *Brain. Behav. Immun.* **49**, 119–129. (doi:10.1016/j.bbi.2015.04.018)
66. Iyer A, Zurolo E, Prabowo A, Fluiter K, Spliet WGM, van Rijen PC, Gorter JA, Aronica E. 2012 MicroRNA-146a: a key regulator of astrocyte-mediated inflammatory response. *PLoS ONE* **7**, e44789. (doi:10.1371/journal.pone.0044789)
67. Xu WD, Lu MM, Pan HF, Ye DQ. 2012 Association of microRNA-146a with autoimmune diseases. *Inflammation* **35**, 1525–1529. (doi:10.1007/s10753-012-9467-0)
68. Cui JG, Li YY, Zhao Y, Bhattacharjee S, Lukiw WJ. 2010 Differential regulation of Interleukin-1 receptor-associated Kinase-1 (IRAK-1) and IRAK-2 by microRNA-146a and NF- $\kappa$ B in stressed human astroglial cells and in Alzheimer disease. *J. Biol. Chem.* **285**, 38 951–38 960. (doi:10.1074/jbc.M110.178848)
69. Cogswell JP *et al.* 2008 Identification of miRNA changes in Alzheimer's disease brain and CSF yields putative biomarkers and insights into disease pathways. *J. Alzheimer's Dis.* **14**, 27–41. (doi:10.3233/JAD-2008-14103)
70. Sethi P, Lukiw WJ. 2009 Micro-RNA abundance and stability in human brain: specific alterations in Alzheimer's disease temporal lobe neocortex. *Neurosci. Lett.* **459**, 100–104. (doi:10.1016/j.neulet.2009.04.052)
71. Kiko T, Nakagawa K, Tsuduki T, Furukawa K, Arai H, Miyazawa T. 2014 MicroRNAs in plasma and cerebrospinal fluid as potential markers for Alzheimer's disease. *J. Alzheimer's Dis.* **39**, 253–259. (doi:10.3233/JAD-130932)
72. Müller M, Kuiperij HB, Claassen JA, Küsters B, Verbeek MM. 2014 MicroRNAs in Alzheimer's disease: differential expression in hippocampus and cell-free cerebrospinal fluid. *Neurobiol. Aging* **35**, 152–158. (doi:10.1016/j.neurobiolaging.2013.07.005)
73. Dong H *et al.* 2015 Serum MicroRNA profiles serve as novel biomarkers for the diagnosis of Alzheimer's disease. *Dis. Markers* **2015**, 625659. (doi:10.1155/2015/625659)
74. Ghosh A *et al.* 2014 Rapid isolation of extracellular vesicles from cell culture and biological fluids using a synthetic peptide with specific affinity for heat shock proteins. *PLoS ONE* **9**, e110443. (doi:10.1371/journal.pone.0110443)
75. Saucier D *et al.* 2019 Identification of a circulating miRNA signature in extracellular vesicles collected from amyotrophic lateral sclerosis patients. *Brain Res.* **1708**, 100–108. (doi:10.1016/j.brainres.2018.12.016)
76. Hua YJ, Tang ZY, Tu K, Zhu L, Li YX, Xie L, Xiao HS. 2009 Identification and target prediction of miRNAs specifically expressed in rat neural tissue. *BMC Genomics* **10**, 214. (doi:10.1186/1471-2164-10-214)
77. Liu G, Detloff MR, Miller KN, Santi L, Houllé JD. 2012 Exercise modulates microRNAs that affect the PTEN/mTOR pathway in rats after spinal cord injury. *Exp. Neurol.* **233**, 447–456. (doi:10.1016/j.expneurol.2011.11.018)
78. Hoss AG *et al.* 2015 MiR-10b-5p expression in Huntington's disease brain relates to age of onset and the extent of striatal involvement. *BMC Med. Genomics* **8**, 1–14. (doi:10.1186/s12920-015-0083-3)
79. Varendi K, Kumar A, Härma MA, Andressoo JO. 2014 MIR-1, miR-10b, miR-155, and miR-191 are novel regulators of BDNF. *Cell. Mol. Life Sci.* **71**, 4443–4456. (doi:10.1007/s00018-014-1628-x)
80. Li Y, Yui D, Luikart BW, McKay RM, Li Y, Rubenstein JL, Parada LF. 2012 Conditional ablation of brain-derived neurotrophic factor-TrkB signaling impairs striatal neuron development. *Proc. Natl. Acad. Sci. USA* **109**, 15 491–15 496. (doi:10.1073/pnas.1212899109)
81. Buchman AS, Yu L, Boyle PA, Schneider JA, De Jager PL, Bennett DA. 2016 Higher brain BDNF gene expression is associated with slower cognitive decline in older adults. *Neurology* **86**, 735–741. (doi:10.1212/WNL.0000000000002387)
82. Sadanand A, Janardhanan A, Vanisree AJ, Pavai T. 2018 Neurotrophin Expression in lymphocytes: a powerful indicator of degeneration in Parkinson's disease, amyotrophic lateral sclerosis and ataxia. *J. Mol. Neurosci.* **64**, 224–232. (doi:10.1007/s12031-017-1014-x)
83. Ślusarz A, Pulakat L. 2015 The two faces of miR-29. *J. Cardiovasc. Med.* **16**, 480–490. (doi:10.2459/JCM.0000000000000246)
84. Mundalil VM *et al.* 2014 Serum microRNA profiles in children with autism. *Mol. Autism* **5**, 40. (doi:10.1186/2040-2392-5-40)
85. Moreau MP, Bruse SE, David-Rus R, Buyske S, Brzustowicz LM. 2011 Altered microRNA expression profiles in postmortem brain samples from individuals with schizophrenia and bipolar disorder. *Biol. Psychiatry* **69**, 188–193. (doi:10.1016/j.biopsych.2010.09.039)
86. Leidinger P *et al.* 2013 A blood based 12-miRNA signature of Alzheimer disease patients. *Genome Biol.* **14**, R78. (doi:10.1186/gb-2013-14-7-r78)
87. dos Santos MCT *et al.* 2018 miRNA-based signatures in cerebrospinal fluid as potential diagnostic tools for early stage Parkinson's disease. *Oncotarget* **9**, 17 455–17 465. (doi:10.18632/oncotarget.24736)

88. Pallarès-Albanell J, Zomeño-Abellán MT, Escaramís G, Pantano L, Soriano A, Segura MF, Martí E. 2019 A high-throughput screening identifies microRNA inhibitors that influence neuronal maintenance and/or response to oxidative stress. *Mol. Ther. Nucleic Acids* **17**, 374–387. (doi:10.1016/j.omtn.2019.06.007)
89. Kruman II, Pedersen WA, Springer JE, Mattson MP. 1999 ALS-linked Cu/Zn-SOD mutation increases vulnerability of motor neurons to excitotoxicity by a mechanism involving increased oxidative stress and perturbed calcium homeostasis. *Exp. Neurol.* **160**, 28–39. (doi:10.1006/exnr.1999.7190)
90. Bao N, Fang B, Lv H, Jiang Y, Chen F, Wang Z, Ma H. 2018 Upregulation of miR-199a-5p protects spinal cord against ischemia/reperfusion-induced injury via downregulation of ECE1 in Rat. *Cell. Mol. Neurobiol.* **38**, 1293–1303. (doi:10.1007/s10571-018-0597-2)